Tellus (2007), 59, 685–697
Printed in Singapore. All rights reserved

TELLUS

A comparison of the transport of long-lived atmospheric trace gas species from two advection schemes incorporated into an atmospheric general circulation model

By H. STRUTHERS[1]*, W. ALLAN[2], D. C. LOWE[2] and B. BHASKARAN[3], [1]*National Institute of Water and Atmospheric Research, Lauder 9352, New Zealand;* [2]*National Institute of Water and Atmospheric Research, Wellington, New Zealand;* [3]*Met Office Hadley Centre, Exeter, United Kingdom*

(Manuscript received 18 October 2006; in final form 22 May 2007)

ABSTRACT

Two tracer advection schemes have been compared using an atmospheric chemical transport model based on the U.K. Met Office's Unified Model (UM). Two experiments were carried out. The first used an inert calibration tracer (SF_6) whilst the second experiment modelled two methane (CH_4) carbon isotopic species. In both experiments, tracer emissions were prescribed at the Earth's surface. Results from both experiments suggest that the global distribution of long lived trace species in the troposphere is not strongly dependent on the choice of the advection scheme. This is attributed to the fact that turbulent boundary layer mixing and vertical transport by convection, in addition to advection play a role in determining the large-scale tracer distribution in the troposphere. For the SF_6 experiment, results from the UM were comparable to results from other transport models using the same experimental protocol. The UM's default, total variation diminishing (TVD) advection scheme produced low values of marine boundary layer mixing ratios compared with other models and measurements. This was attributed to the TVD scheme being too diffusive resulting in unrealistically fast vertical transport. Comparisons between measured and modelled CH_4 profiles in the stratosphere clearly shows that the vertical transport in the TVD scheme is too fast.

1. Introduction

When comparing Chemistry Transport Model (CTM) results with measured data, it is important to understand how the details of the numerical scheme used to advect trace species affect the results from the model in question. The Atmospheric Tracer Transport Model Intercomparison Project (TransCom, http://www.purdue.edu/transcom/) experiments were designed to address the question of uncertainty in the simulated atmospheric transport of trace species within a number of CTMs. The TransCom 1 experiment (Rayner and Law, 1995; Law et al., 1996) involved the intercomparison of results from 12 different three-dimensional atmospheric transport models each transporting two CO_2 tracer fields (fossil-fuel and annually balanced biotic component). The surface emission fields and initial CO_2 concentrations were prescribed and fixed to be the same for all models. The modelled CO_2 distributions showed broadly similar concentration distributions but a large range in the transport efficiency. Surface interhemispheric exchange times in the fossil-fuel experiment varied by a factor of 2. Results indicate that the vertical transport in the models is an important factor influencing the hemispheric CO_2 gradient at the surface.

For the biosphere experiment, surface annual mean and seasonal cycles from the models were compared with surface CO_2 measurements from the National Oceanic and Atmospheric Administration/Global Monitoring Division (NOAA/GMD). As with the fossil-fuel experiment, a range of model responses was found. This study demonstrated that hemispheric carbon budgets derived from model inversions carry an extra uncertainty associated with uncertainties in model transport.

The TransCom 2 experiment (Denning et al., 1999) used SF_6 as the calibration tracer and more comprehensive flux diagnostics were retained for comparison. Eleven models were included in this study and model results were compared with a number of

*Corresponding author.
e-mail: h.struthers@niwa.co.nz
DOI: 10.1111/j.1600-0889.2007.00295.x

observational data sets. The observed meridional SF_6 gradient was reasonably well simulated by the models. Results reinforce the conclusion from Law et al. (1996) that vertical transport rather than meridional transport is the dominant control on the modelled meridional gradient at the surface.

A tracer transport general circulation model based on the U.K. Met Office's Unified Model (UM) was not included in either of the TransCom experiments. Tracer transport in the UM was studied by Gregory and West (2002). They compared the transport of water vapour by the Heun advection scheme, based on finite differences as described by Cullen and Davis (1991), with a second advection formulation based on the flux-limited total variation diminishing (TVD) scheme of Roe (1985). They found the vertical transport of water vapour in the stratosphere using TVD was too fast compared to the satellite based, Halogen Occultation Experiment (HALOE) measurements. This was attributed to the scheme, as implemented in the UM, being too diffusive. The Heun scheme gave a better comparison with measurements. They also introduced a new tracer advection formulation based on an extended Non-Oscillatory Integrally Reconstructed Volume-Averaged Numerical Advection (eNIRVANA) scheme (Leonard et al., 1995). Preliminary results from the eNIRVANA scheme suggested that it produced more realistic stratospheric vertical transport than the TVD scheme. This was attributed to the eNIRVANA scheme being less diffusive than the TVD scheme.

In this paper, we compare the atmospheric transport of long-lived tracers using the eNIRVANA and the TVD advection formulations in the UM. A modification of the UM has been developed and used for the study of surface emission and transport of methane (CH_4) carbon isotopic species and to assist in the interpretation of methane measurements made at remote marine boundary layer sites in the southern hemisphere (Lowe et al., 2004; Allan et al., 2005, 2007). In this work, we examine how the model advection schemes influence the model results, as it is important to understand this before drawing conclusions from model/measurement comparisons.

Two model experiments were completed. The first follows the TransCom 2 protocol of Denning et al. (1999) using SF_6 as the calibration tracer. This allows us to compare UM results using two different tracer advection schemes (TVD and eNIRVANA) with results from the 11 models that took part in the TransCom2 study. In the second experiment, we compare the CH_4 fields generated by the UM using eNIRVANA and TVD. The CH_4 in the model is chemically active being destroyed in situ via oxidation by OH radicals. This process is modelled in the UM using a fixed climatology of OH radicals derived from results of a full atmospheric chemistry model.

2. Description of the dynamical model and the eNIRVANA and TVD advection schemes

The results described in this paper are based on integrations of the Met Office UM (Cullen, 1993), a general circulation model widely used for both short range weather forecasting and long range climate prediction studies. The UM was configured with a horizontal resolution of 2.5° (latitude), 3.75° (longitude) and 19 vertical levels, with the top level of the model at approximately 4 hPa. The HadAM3 set of physical parametrizations (Pole et al., 2000) developed by the Met Office Hadley Centre (METO-HC) was used to represent physical processes not described by the dynamical core of the model. The HadAM3 configuration includes a full suite of physical parametrizations describing subgrid scale mixing, large-scale and convective clouds and precipitation, boundary layer and surface processes and gravity wave propagation and breaking.

2.1. The total variation diminishing advection scheme

The UM includes a positive definite tracer advection scheme based on the TVD formulation described by Cullen and Barnes (1997). The TVD advection algorithm is based on the formulation of Roe (1985) and uses operator splitting to reduce the full three-dimensional operation to a sequence of three one-dimensional steps. Details of the TVD algorithm can be found in Gregory and West (2002). The scheme provides a choice of two monotonic limiters, the so-called SUPERBEE and VAN LEER limiters. The TVD scheme is used as the default advection scheme for tracers in the UM. Water vapour in the model is advected using the Heun scheme (Cullen and Davis, 1991). The Heun advection scheme as implemented in the UM is not positive definite, which is a requirement for the advection of tracers.

2.2. The extended Non-Oscillatory Integrally Reconstructed Volume-Averaged Numerical Advection (eNIRVANA) scheme

A version of the eNIRVANA advection algorithm was coded for inclusion in the UM by Gregory and West (2002) as an alternative to the TVD tracer advection scheme. The eNIRVANA scheme also uses operator splitting to reduce the full three-dimensional problem to a sequence of one-dimensional steps. The one-dimensional methods used for calculating the advection increments are closely related to van Leer's extension of Godunov's method (Godunov, 1959; van Leer, 1977). The scheme as implemented by Gregory and West (2002) is equivalent to a scheme that uses a piecewise quartic subcell distribution of the tracer field. Monotonicity is enforced by limiting the interpolation so that it does not introduce any new extrema in the cell average tracer distribution (Leonard et al., 1995). For Courant numbers less than one, the method is closely related to the universal limiter described by Leonard (1991). As with the TVD model setup, the modelled water vapour is advected using the Heun scheme.

2.3. Turbulent boundary layer mixing and vertical transport of tracers by convection

Mixing in the boundary layer of trace species emitted at the Earth's surface is important for determining the large-scale distribution of those species in the atmosphere (Law et al., 1996). In addition to advection, two further processes affecting tracer concentrations are modelled in the UM: (i) rapid turbulent mixing of tracers in the atmospheric boundary (near surface) layer and (ii) vertical transport due to convection. Both processes can have a significant effect on the structure of the global tracer distributions for tracers with a surface source.

Turbulent tracer fluxes for levels above the bottom model layer are parametrized using a 'local mixing' type first-order turbulent closure approximation:

$$\frac{F_X}{\rho} = -K_X \frac{\partial X}{\partial z}, \tag{1}$$

where F_X is the mean turbulent flux of the conserved quantity X, ρ is the atmospheric density, and K_X is the turbulent mixing coefficient for the quantity X. K_X is in general a function of the mixing length, the local wind shear and atmospheric stability. The functional dependence of K_X is specified empirically within the model (Smith, 1993):

$$K_X = \mathcal{L}_X \mathcal{L}_M f_X(R_i) \left| \frac{\partial v}{\partial z} \right|. \tag{2}$$

$\mathcal{L}_X$ and $\mathcal{L}_M$ are the tracer and momentum neutral mixing lengths, respectively, and are estimated using the Blackader formula (Blackader, 1962). The stability function f_X is specified in terms of the Richardson number (R_i) (Smith, 1993) and $|\partial v/\partial z|$ is the wind shear.

The boundary layer depth in the model generally lies between the third and fifth model level (~600–2000 m altitude). The turbulent mixing falls to near zero above the boundary layer and is switched off in the model above the fifth model level.

The UM convection scheme represents the transport of heat, moisture, momentum and tracers associated with cumulus convection occurring in a model gridbox. The same scheme is used to represent both precipitating and non-precipitating convection. The convection scheme models an ensemble of cumulus clouds within a gridbox as a single entraining–detraining plume. Cloud base closure is parametrized using the convective available potential energy (CAPE) closure approximation (Fritsch and Chappell, 1980). The initial value of the tracer mixing ratio in the ascending parcel is set to the tracer mixing ratio at the level at which convection is initiated. The tracer in the updraft is modified as it ascends through entrainment of surrounding air whilst the tracer amounts in the air surrounding the convective parcel are modified through detrainment (forced and mixing) and subsidence. Entrainment and detrainment coefficients used to parametrize the exchange of tracers are the same as used for entrainment and detrainment of water vapour and potential temperature. No treatment of tracer removal by convective precipitation is included. Terminal detrainment of the tracer at the top of the convective plume is modelled by allowing a portion of the tracer in the convective parcel to be detrained into the model layer above which the convection terminates.

3. SF_6 experiment

3.1. Model setup

The model setup for the SF_6 experiment follows the protocol of the TransCom 2 experiment detailed by Denning et al. (1999):

(1) The surface emissions of SF_6 are prescribed at each gridpoint of the model. Values were interpolated from data supplied through the TransCom 2 experiment. These were derived from the global emission estimates of Levin and Hesshaimer (1996) and distributed geographically according to power usage and population density. Total emissions vary as a function of time with a repeating annual cycle.

(2) The initial model SF_6 field was set to a uniform global molar mixing ratio of 2.06 parts per trillion (ppt). The model was initialized on January 1, 1989 and run for 5 yr. Results from the last year of the run were used in the analysis.

(3) No sink of SF_6 was included. This is a fair assumption over the 5 yr of the model integration given the estimated mean lifetime of SF_6 in the atmosphere is over 3000 yr.

(4) The global sea-ice and surface temperature (GISST) data set was used as the surface boundary forcing in the UM. The data set contains monthly normals of SST and sea ice, with the same annual cycle being repeated for the 5 yr of the model run.

3.2. Results and discussion

Figure 1 compares measurements of SF_6 made at 24 remote marine boundary layer (MBL) sites (see Table 1) with the SF_6 mixing ratio in the lowest layer of the model interpolated to the

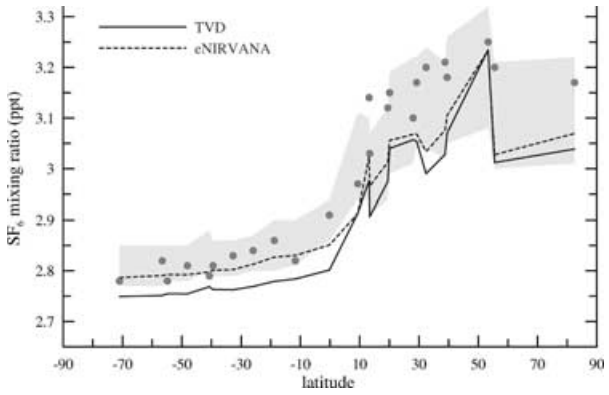

Fig. 1. Simulated and measured 1993 annual mean SF_6 surface mixing ratio (ppt) at the 24 marine boundary layer sites listed in table 1. The grey shaded region shows the range of model values for the same locations from Denning et al. (1999).

Table 1. Simulated and measured SF_6 mole fractions (ppt). Measured values from Denning et al. (1999). Model values have been adjusted according to the revised emissions estimates as described in the text. * indicates these locations are not considered marine boundary locations and are therefore not used in Fig. 1

Station	Latitude	Longitude	Observation (ppt)	UM (TVD) (ppt)	UM (eNIRVANA) (ppt)
Neumayer	−71.0	−8.0	2.78	2.75	2.79
Atlantic transect 12	−56.6	9.1	2.82	2.75	2.79
Tierra del Fuego	−54.9	−68.5	2.78	2.75	2.79
Atlantic transect 11	−48.1	9.1	2.81	2.75	2.79
Cape Grim, Tasmania	−40.7	144.7	2.79	2.77	2.80
Atlantic transect 10	−39.5	7.9	2.81	2.76	2.80
Atlantic transect 9	−32.7	8.6	2.83	2.76	2.80
Atlantic transect 8	−25.9	10.1	2.84	2.77	2.81
Atlantic transect 7	−18.8	8.0	2.86	2.78	2.83
Atlantic transect 6	−11.7	−7.3	2.82	2.78	2.83
Atlantic transect 5	−0.2	−18.5	2.91	2.80	2.85
Atlantic transect 4	9.4	−23.7	2.97	2.91	2.91
Barbados	13.2	−59.4	3.14	2.98	3.02
Guam	13.4	144.8	3.03	2.91	2.97
Kumukahi, Hawaii	19.5	−154.8	3.12	2.98	3.01
Atlantic transect 3	20.1	−21.2	3.15	3.04	3.06
Izana	28.0	−16.0	3.10	3.06	3.07
Atlantic transect 2	29.2	−17.1	3.17	3.05	3.07
Bermuda	32.4	−64.7	3.20	2.99	3.03
Azores	38.8	−27.1	3.21	3.03	3.08
Atlantic transect 1	39.5	−14.3	3.18	3.07	3.11
Mace Head, Ireland	53.3	−9.9	3.25	3.23	3.23
Cold Bay, Alaska	55.2	−162.7	3.20	3.01	3.03
Alert	82.5	−62.5	3.17	3.04	3.07
North Carolina Tower*	35.4	−77.4	3.41	3.18	3.21
Tae Ahn Peninsula*	36.7	126.1	3.25	3.38	3.32
Utah*	39.9	−113.7	3.21	3.02	3.03
Wisconsin Tower*	45.9	−90.3	3.31	3.28	3.35
Hungary*	47.0	16.4	3.42	3.42	3.42
Fraserdale*	50.0	−82.0	3.25	3.09	3.15

same locations. The model values are annual means from the last year of the model integration (1993). The measured values were extrapolated to the intercomparison year (1993) assuming a linear trend of 0.202 ppt yr^{-1}. The modelled values are scaled using the prescription of Denning et al. (1999) to correct for the overestimate of the initial mole fraction of SF_6 in the model:

$$\chi_{\mathrm{adj}} = 2.06 + 0.936 \times (\chi - 2.06) \quad \text{(ppt)}. \tag{3}$$

The grey shaded region of figure 1 indicates the range of model values for the 11 different models included in the intercomparison of Denning et al. (1999). Results from the TVD advection run (solid line) lie below the observations and all the other model values in the southern hemisphere. The eNIRVANA results lie above the TVD results for all MBL stations considered here. The lower SF_6 mixing ratios from the TVD scheme suggest faster transport of SF_6 out of the boundary layer in this model compared to the eNIRVANA scheme. The amount of turbulent boundary layer mixing and convective transport of tracers is not expected to significantly differ between the two runs. This indicates that the different advection schemes are responsible for the differing MBL SF_6 concentrations seen in Fig. 1. Slower vertical transport by the eNIRVANA scheme compared with the TVD scheme observed in this experiment is consistent with the slower vertical advection observed by Gregory and West (2002) in their stratospheric model experiments. The eNIRVANA surface concentrations are in general higher than those for the TVD scheme over the whole globe (not shown). Isolated exceptions occur near high emission sources (North America and Europe). The global surface concentration patterns from the TVD and eNIRVANA runs are similar to the results from the ANU and GISS-UVic models in Denning et al. (1999).

The northern hemispheric MBL sites are underestimated by both advection schemes. Denning et al. (1999) found two clusters of model results in the surface mixing ratio comparisons. One

group of models reproduced the meridional gradient in the remote MBL but overestimated surface mixing ratios particularly in the vicinity of emission maxima. The second group tended to underestimate the MBL meridional gradient but gave a better match at continental locations. Our results here indicate that the UM based models fall into the second category of models, underestimating the MBL meridional gradient but giving a reasonably good match to observations at continental locations.

Comparison with other TransCom 2 model results and surface SF_6 measurements suggest that the model using the eNIRVANA scheme is producing more realistic surface concentrations.

Figure 2 shows the zonal mean SF_6 mixing ratio interpolated to six pressure levels (1000, 700, 500, 300, 200 and 50 hPa) from the TVD and eNIRVANA runs. The 1000 hPa curve shows similar results to the MBL results from Fig. 1 with the eNIRVANA scheme consistently producing slightly higher (∼0.05 ppt) mixing ratios over the whole latitude range. This is true also of the 700, 500 and 300 hPa curves. The peak in the SF_6 mixing ratio around 45°N at the 1000 hPa level associated with peak northern mid-latitude emissions is smoothed out in higher levels reflecting the horizontal mixing of air as the emitted tracer ascends. Above 200 hPa the SF_6 concentration in the eNIRVANA run starts to drop significantly compared to that of the TVD simulation. The eNIRVANA concentration drops below the TVD results at 200 and 50 hPa indicating less of the SF_6 emitted at the surface has been transported to the upper troposphere and stratosphere by the eNIRVANA scheme at the end of the 5 yr model integration. The corollary to this is that the higher mixing ratios of SF_6 in the lower and middle troposphere from the eNIRVANA scheme relative to the TVD scheme are also a result of slower vertical advection of the tracer from the surface. Results in Fig. 2 suggest that it is the difference in the speed of the vertical advection that causes the differences in tracer distributions. In the lower and middle troposphere, the differences between the two schemes are relatively uniform in latitude. If the parametrization of the convective transport was causing significant differences in the tracer distributions between the two runs, we would expect the zonal mean differences to be greater in the tropics where convection is strongest.

The parametrization of boundary layer turbulence can be ruled out as the major cause of the differences between the TVD and eNIRVANA results seen in Fig. 2. This parametrization is only applied to the lowest five layers of the model. If the turbulent mixing in the boundary layer was the greatest difference between the two runs, we would then expect any concentration differences to be greatest in the lowest levels of the model, which is not the case.

One point to note is that both the TVD and eNIRVANA schemes are designed to conserve tracer mass and indeed the global SF_6 masses at the end of the two runs differ by less than 0.1% from the theoretical atmospheric burden of SF_6 based on the initial conditions and prescribed emission rates integrated over the length of the simulation. This confirms that the

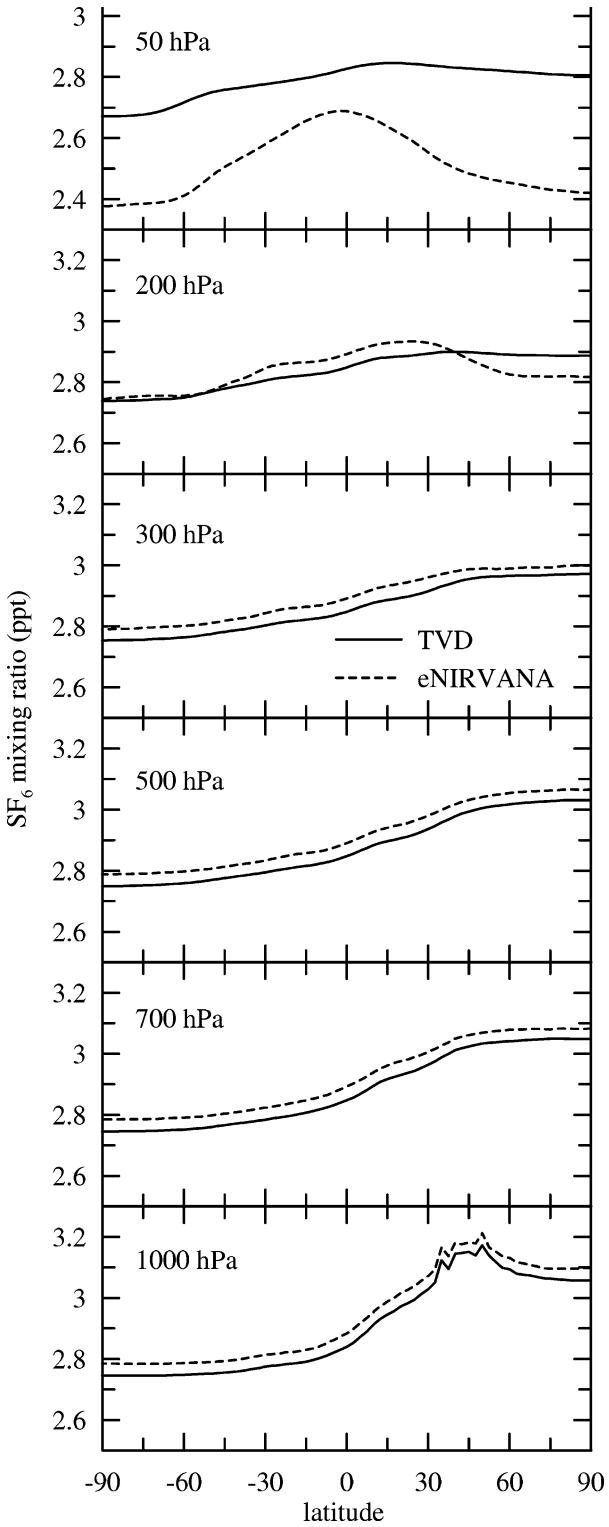

Fig. 2. Modelled 1993 annual and zonal mean SF_6 mixing ratio (ppt) on a selection of pressure surfaces from the TVD and eNIRVANA UM models. Note the change in scale on the *y*-axis of the top panel.

differences seen in Figs. 1 and 2 are differences in the distribution of the SF_6 tracer as opposed to an artefact arising from some numerical loss of tracer in one of the advection schemes.

Long-lived tracers with steadily increasing tropospheric concentrations produce characteristic stratospheric distributions, related to the large-scale Brewer–Dobson circulation present in the stratosphere (Finlayson-Pitts and Pitts, 2000; Brasseur and Solomon, 2005). Typically on a given pressure surface in the stratosphere, tracers of this type have a peak in concentration in the tropics where the tropical upwelling occurs and lower concentrations in the high latitudes associated with descent of air in the winter polar vortices. The eNIRVANA results at 50 hPa show the qualitative behaviour one would expect from a tracer of this type, whereas the TVD curve has no tropical peak. This indicates that the TVD scheme is not producing a realistic simulation of the stratospheric distribution of the SF_6 tracer. The UM configuration used here has a low vertical resolution in the stratosphere so cannot be expected to capture the stratospheric circulation very well, but the model using the eNIRVANA scheme still produces a reasonably realistic stratospheric distribution.

We calculated the interhemispheric exchange time-scale (τ_{ex}) using the four methods described in Denning et al. (1999) who assume a two-box (northern and southern hemisphere) model of the atmosphere. Results are given in Table 2 along with the range of model results found in the TransCom 2 experiments and the exchange time-scale derived from the Atlantic transect measurements. The exchange time-scales for the TVD and eNIRVANA models lie near the middle of the range of model time-scales for all four of the time-scale calculations, and both results also compare well with the time-scale derived from measurements. The differences between the TVD and eNIRVANA time-scales are relatively small compared to the intermodel differences seen in the TransCom2 results of Denning et al. (1999).

Surface mixing ratios and transport efficiencies from the UM models (TVD and eNIRVANA) are relatively similar. The largest differences between the TVD and eNIRVANA results are in the upper troposphere and stratosphere where the inversion of the temperature gradient means there is little or no convection or turbulent mixing and the vertical transport of tracers is dominated by vertical advection, which highlights the differences between the two schemes. As seen by Gregory and West (2002), the TVD scheme's vertical transport is too fast due to the numerical diffusiveness of the scheme.

Table 2. Interhemispheric exchange times (in yr). S-S (steady state) values inferred from transect measurements (see Table 1)

	Oct/Nov	Annual		
	S-S τ_{ex}	τ_{ex} (1-D)	τ_{ex} (2-D)	τ_{ex} (3-D)
UM (TVD)	1.25	1.38	1.30	0.75
UM (eNIRVANA)	1.22	1.23	1.33	0.72
TransCom2 minimum	0.76	0.77	0.94	0.55
TransCom2 maximum	1.97	2.03	2.05	1.26
Observations	1.34			

4. Methane experiment

4.1. Model setup

The same dynamical model used for the SF_6 experiment described in the previous sections was applied to examine the emission, transport and in situ removal of two methane carbon isotopic species ($^{12}CH_4$ and $^{13}CH_4$). Preliminary results from this setup of the model have been described in papers comparing measurements of methane mixing ratio and isotopic fraction at remote southern hemisphere MBL sites with model estimates (Lowe et al., 2004; Allan et al., 2005).

The model setup for the CH_4 experiment follows the protocol of the International Geosphere-Biosphere Program Global Atmospheric Methane Synthesis (GAMeS) scenario (S. Houweling, personal communication, 2001).

(1) CH_4 emissions are specified at each surface gridpoint of the model. The emission values at each point are the sum of 10 emission terms (biomass burning, rice cultivation, termites, bogs, swamps, coal, oil, gas, animals and landfills) and one sink (removal by soil microbes). The biomass burning, rice cultivation, bogs, swamps and soil sink terms vary on a monthly basis. The other terms do not vary temporally. The total source within the model strength is 580 Tg yr^{-1}. The $\delta^{13}C$ values for the methane sources were assigned according to the GAMeS protocol (see Table 3. The $\delta^{13}C$ ratio is defined as:

$$\delta^{13}C \equiv \left(\left[^{13}CH_4\right] / \left[^{12}CH_4\right] - R_0\right) / R_0, \quad (4)$$

where $R_0 = (^{13}C/^{12}C)PDB$ has an accepted value of 0.0112372 for the isotope standard, peedee belemnite (PDB) (Craig, 1957).

(2) To speed up the convergence of the modelled methane fields to steady state, the TVD model was initialized using zonally and vertically uniform methane fields with the latitudinal gradient of the $^{12}CH_4$ field fitted to surface data of the NOAA/GMD network (ftp://ftp.cmdl.noaa.gov/ccg/ch4/). The $\delta^{13}C$ value was initially set to a globally uniform value of $-47‰$. The final state of the TVD run was used as the initial condition for the eNIRVANA run of the model (see Fig. 3).

(3) The major process for removal of methane from the atmosphere is reaction with OH radicals: ($CH_4 + OH \rightarrow CH_3 + H_2O$). This reaction was modelled in the UM using an OH distribution derived independently from results of the MATCH atmospheric chemical model (Rasch et al., 1997). The OH kinetic isotope effect (KIE) was assumed to be fixed at $-3.9‰$ (Saueressig et al., 2001). The rate constant for the reaction of OH with CH_4 was calculated using the expression given by Sander et al. (2003): $k_{12} = 2.45 \times 10^{-12} \exp(-1775/T)$.

(4) Stratospheric removal rates of methane are supplied as part of the GAMeS protocol. In this case, the removal rates rather

Table 3. Methane source strengths and δ^{13}C values from the GAMeS scenario. Note that the soil sink is a negative source with δ^{13}C in the removal flux given by the atmospheric value (−47‰) adjusted for fractionation by −22‰

Source	Source strength (Tg yr^{-1})	δ^{13}C (‰)	Monthly varying
Animals	98.0	−62.0	No
Biomass burning	49.4	−25.0	Yes
Bogs	40.3	−64.3	Yes
Coal	41.7	−35.2	No
Gas	48.0	−40.2	No
Landfills	47.7	−51.1	No
Oil	34.5	−40.1	No
Rice cultivation	80.0	−62.7	Yes
Swamps	121.7	−54.8	Yes
Termites	19.3	−57.0	No
Soil sink	−37.9	−69.0	Yes
Total emissions excluding soil sink	580.6		

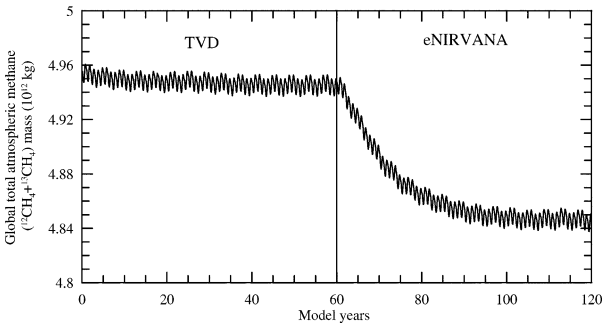

Fig. 3. Time-series of total atmospheric burden of methane ($^{12}CH_4$ + $^{13}CH_4$) from the TVD and eNIRVANA UM model runs.

than the reaction rate constants are provided. Three stratospheric loss processes are modelled: reaction with OH, reaction with O(^{1}D), and reaction with Cl radicals. The KIE for the reaction with Cl is particularly high (1.066) which has a strong effect on the methane fractionation.

(5) The tropopause boundary between tropospheric and stratospheric removal rates is set at 100 hPa in the tropics (30°S–30°N), and at 200 hPa elsewhere.

(6) We used a composite 4-yr El Niño and La Niña sea surface temperature (SST) and sea ice cycle developed by Spencer et al. (2004) which was repeated over the whole period of the integration.

(7) Both the TVD and eNIRVANA simulations were run for 60 model years to allow an equilibrium to be established within the model between the surface emissions and in situ removal of methane.

4.2. Results and discussion

Time-series of the total atmospheric mass of methane ($^{12}CH_4$ + $^{13}CH_4$) for both runs are shown in Fig. 3. The seasonal cycle in global CH_4 mass is evident in Fig. 3. This results from the interaction between seasonal cycles of the surface emission and in situ removal. A smaller 4 yr cycle related to the imposed 4 yr ENSO SST cycle is also present.

The equilibrium global masses from the model (TVD = 4950 Tg, eNIRVANA = 4850 Tg) compare well with the Intergovernmental Panel on Climate Change (IPCC) estimate of the total atmospheric burden of CH_4 of 4850 Tg for 1998 (Prather et al., 2001), but this comparison should be treated with some caution as the GAMeS scenario has not been designed to simulate the real transient behaviour of the atmosphere through the 1990s. For a system in steady state, the lifetime of a species is given by the total burden divided by the total emissions (equal to the total loss at steady state). The TVD (8.53 yr) and eNIRVANA (8.36 yr) values compare well with the IPCC estimate for 1998 of 8.4 yr, but again this comparison should be treated with some caution given the limitations of the GAMeS scenario and the fact that the model was run to steady state, unlike the real atmosphere.

The steady state global CH_4 burden is 100 Tg less in the eNIRVANA case than in the TVD case. This difference arises because of the slower cross-tropopause transport of CH_4 in the eNIRVANA scheme, particularly at extra-tropical latitudes. Details are discussed later in this section. The rates of destruction of CH_4 by OH, O(^{1}D) and Cl in the stratosphere are prescribed in the GAMeS protocol. These rates are identical for both the TVD and eNIRVANA runs, but the eNIRVANA scheme transports CH_4 more slowly upwards into and through the stratosphere. Consequently, the total stratospheric burden of CH_4 is somewhat less in the eNIRVANA case. This can be seen in Fig. 4 (top two left-hand panels), which compare the zonal mean 200 and 50 hPa mixing ratio profiles for the two runs.

Figure 4 compares the TVD and eNIRVANA meridional profiles of CH_4 mixing ratio and δ^{13}C over the same pressure levels as shown in Fig. 2 for the SF_6 experiment. We initially consider

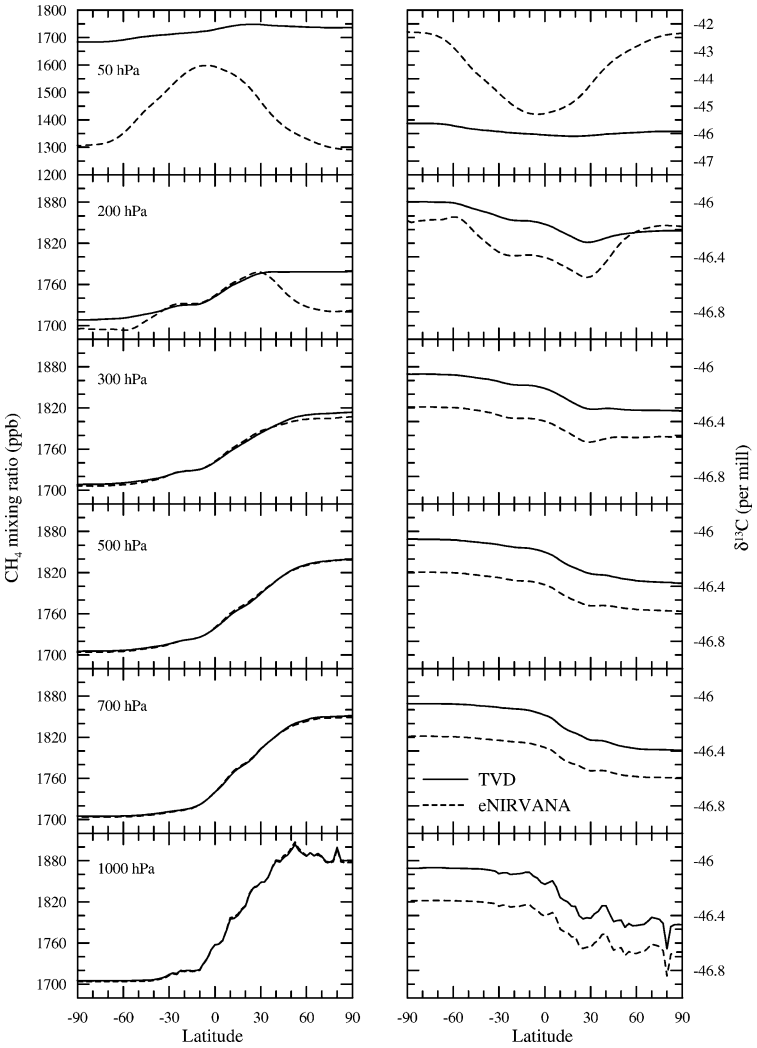

Fig. 4. Zonal mean CH_4 ($^{12}CH_4 + {}^{13}CH_4$) mixing ratio (ppb) and $\delta^{13}C$ (‰) on a selection of pressure surfaces. Values are averaged over the last 4 yr of the model runs. Note the change in scale on the *y*-axis of the top panels.

only the mixing ratio results, and will discuss the $\delta^{13}C$ results later in this section. The mixing ratio profiles for the lower and middle troposphere are very similar for the TVD and eNIRVANA runs, unlike the SF_6 experiment, which showed a difference between the two schemes. The simple methane oxidation chemistry in the model is the cause of the different behaviour for the CH_4 experiment compared to the SF_6 experiment, as it tends to rectify CH_4 perturbations. Figure 5 shows the time-series of CH_4 mixing ratio and $\delta^{13}C$ on the same set of pressure surfaces as previous figures. The values are averages (area weighted) over the region 30°S–60°S and 0–360°E, which was chosen to be well away from the major surface source regions. The time-series show the mean mixing ratio and $\delta^{13}C$ from the time of switching from the TVD to the eNIRVANA advection scheme (year 60 in Fig. 3).

Concentrating on the mixing ratio time-series (left-hand panels), we see that over the first 2 yr there is an increase in the mixing ratios in the lower and middle troposphere followed by a slower reduction to near the starting values. The initial increase in concentration is associated with the change in advection scheme. As shown in the SF_6 experiment, the eNIRVANA scheme manifests slower transport from the boundary layer, so we expect lower and mid tropospheric mixing ratios of CH_4 to increase when switching from the TVD to the eNIRVANA scheme. The slow decrease back to near the starting values seen in Fig. 5 can be attributed to the OH oxidation chemistry. The amount of CH_4 oxidised is proportional to the CH_4 concentration, so as the concentration initially increases due to the change in advection scheme, the rate of CH_4 loss also increases and eventually restores the mixing ratios to values near where they started. The distribution of CH_4 mixing ratios in the mid and lower troposphere when the model has been run to equilibrium are, therefore, under some chemical control. This effect explains why the global average CH_4 burden is 100 Tg less in the eNIRVANA case than in the TVD case. The initial tropospheric mixing ratio increase in Fig. 5 implies trapping of CH_4 in the troposphere that would have gone into the stratosphere in the TVD run. The subsequent decay denotes extra CH_4 destruction, leading to a slightly decreased global CH_4 burden in the eNIRVANA case.

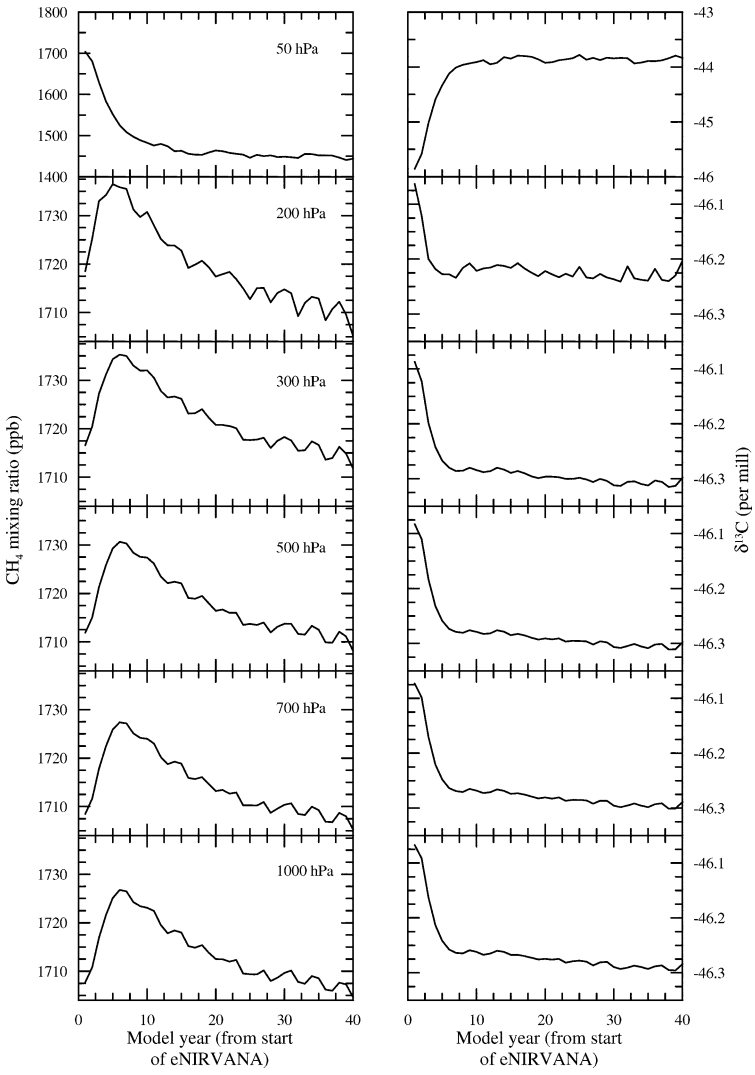

Fig. 5. Time-series of the average CH_4 ($^{12}CH_4 + {}^{13}CH_4$) mixing ratio (ppb) and $\delta^{13}C$ (‰) on fixed pressure surfaces. Averages (latitudinally weighted) are taken over the region 30°S–60°S and 0–360°E. Model years are from the start of the eNIRVANA run (year 60 in Fig. 3).

The situation in the stratosphere is different because the actual rate of CH_4 destruction is specified rather than using the rate equation. Therefore, there is no rectifying effect present and no recovery of the CH_4 from the initial perturbation due to the change in advection scheme (top left-hand panel of Fig. 5). The CH_4 values at 50 hPa fall when changing from the TVD to the eNIRVANA scheme because of the reduction in the cross-tropopause transport as seen in the SF_6 experiment and the slower transport up through the stratosphere.

The $\delta^{13}C$ values derived from the model results behave rather differently to the CH_4 mixing ratios. There is a clear difference between the TVD and eNIRVANA equilibrium values at all levels (right-hand panels of Fig. 4). From the transient behaviour in southern mid-latitudes (right-hand panels of Fig. 5) we see that there is no slow recovery after the initial perturbation due to the change in advection scheme, as was seen in the CH_4 mixing ratio time-series.

The area weighted mean $\delta^{13}C$ of all sources in the GAMeS scenario is $-51.5‰$. As the CH_4 is released from the surface and ages, the $\delta^{13}C$ increases due to the action of the OH sink and, to a lesser extent, the soil sink. The actual $\delta^{13}C$ values for the sources vary with location and therefore surface $\delta^{13}C$ values will be dependent on location and will vary with time as the surface meteorology changes. This has been used to identify episodic events of transport of air masses across tropical convergence zones (Lowe et al., 2004) but for the purposes of this discussion we can reasonably use the global average because of the large spatial and temporal scales considered here.

The chemical rectification effect seen in the CH_4 mixing ratio time-series of Fig. 5 would not be expected to influence the $\delta^{13}C$ significantly because the $\delta^{13}C$ value is essentially the ratio of two CH_4 concentrations, and therefore the rectification effect of the chemistry is cancelled out. The $\delta^{13}C$ results shown in Fig. 4 are consistent with the results from the SF_6 experiment.

The TVD advection scheme is significantly more diffusive than the eNIRVANA scheme resulting in less vertical structure in the resulting model fields. This is discussed below when comparing measured and modelled profiles of CH_4 and $\delta^{13}C$.

4.3. Comparison with measurements

Currently, there are large uncertainties in the estimates of surface methane emissions used for global modelling studies (IPCC, 2001). These large uncertainties in turn create significant uncertainties in the modelled surface values of CH_4 and $\delta^{13}C$ when these emission estimates are applied to models. For example, Mikaloff Fletcher et al. (2004) use an inverse modelling approach based on GLOBALVIEW-CH_4 (National Oceanic and Atmospheric Administration (NOAA), 2001) data product and $^{13}C/^{12}C$ isotopic ratios measured at six NOAA/Climate Monitoring and Diagnostics Laboratory (CMDL) stations in 1998 and 1999 to constrain estimates of surface emissions of methane. They show differences in the modelled CH_4 latitudinal gradient of approximately 50 ppb between the forward simulation based on the *a priori* emissions and the forward simulation based on the *a posterori* emissions. Similarly the difference between the $\delta^{13}C$ in the forward simulation based on the *a priori* emissions and the forward simulation based on the *a posterori* emissions is greater than 0.5‰ over the whole latitude range.

The latitudinal gradients in the surface CH_4 mixing ratio and $\delta^{13}C$ from our model simulations (see bottom panels of Fig. 4) are similar to the model results of Mikaloff Fletcher et al. (2004) when they use their *a priori* emissions estimates. Our model surface gradients are also consistent with the measured gradients shown in Mikaloff Fletcher et al. (2004). The differences in the modelled latitudinal gradients of CH_4 and $\delta^{13}C$ associated with the change from *a priori* to *a posterori* surface emissions shown in Mikaloff Fletcher et al. (2004) are significantly greater than the differences we see when changing from the TVD to the eNIRVANA advection schemes. This would suggest that comparisons between measured and modelled gradients in CH_4 and $\delta^{13}C$ at the surface can not help to discriminate between the TVD or eNIRVANA advection schemes because of the large uncertainties in the surface emissions used in the model.

Comparison of model results with upper air measurements is a robust test of the fidelity of the modelled transport (Denning et al., 1999). Unfortunately, there are few measurements of $\delta^{13}C$ outside the surface boundary layer. Sugawara et al. (1997) measured the vertical profile of CH_4 mixing ratio and $\delta^{13}C$ from air samples collected by balloon flights over Japan in July and August of 1994. Figure 6 compares the measured profiles from Sugawara et al. (1997) with our model results from the gridpoint closest to the measurement location. The model profiles are August means averaged over the last 4 yr of the TVD and eNIRVANA runs. As seen in Fig. 4, the CH_4 mixing ratios in the lower and middle troposphere (below ~10 km) are very similar for the two advection schemes. They also compare very well with observations. The modelled CH_4 profiles in the stratosphere significantly diverge, with the eNIRVANA profile following the observed decrease in mixing ratio with height very well. The TVD profile, on the other hand, shows little decrease in mixing ratio with height, as seen in previous figures. This results from the excessive numerical diffusion inherent in the scheme.

The same picture holds for the $\delta^{13}C$ profiles shown in the right-hand panel of Fig. 6. Both sets of model results are offset to slightly more positive $\delta^{13}C$ values than the observations. This could easily be corrected by using a slightly more positive mean source $\delta^{13}C$. However, it is clear that the TVD profile shows an unrealistic vertical structure with very little increase in $\delta^{13}C$ with height in the stratosphere compared with observations. The model using the eNIRVANA advection scheme gives a more realistic profile.

The comparison with observed profiles in Fig. 6 lends weight to the conclusion that the TVD scheme exhibits excessive numerical diffusion leading to an overly smooth vertical structure for tracer fields with a surface source. This is particularly evident in the stratosphere where vertical transport is dominated

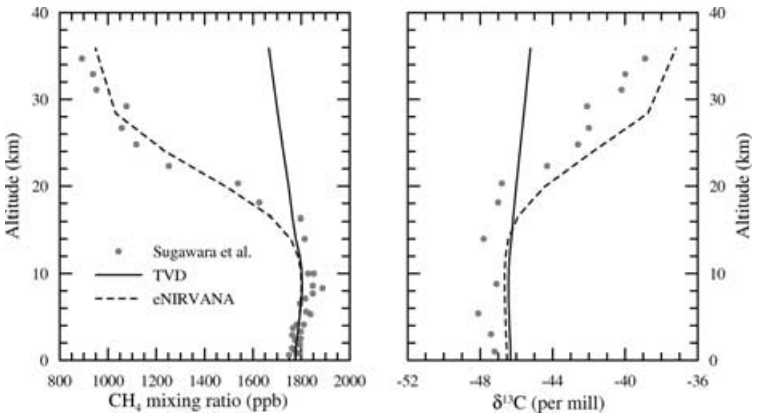

Fig. 6. Comparison of simulated and measured CH_4 ($^{12}CH_4 + {}^{13}CH_4$) mixing ratio (ppb) and $\delta^{13}C$ (‰) over Japan (approximately 40°N, 140°E). Simulated profiles are averages over the last 4 yr of the model integrations (TVD and eNIRVANA) for the closest gridbox to the measurement location.

by advection with little or no contribution from convection or turbulent mixing.

Further evidence supporting this comes from the two-dimensional modelling studies of Bergamaschi et al. (1996) and McCarthy et al. (2003). Both models have a vertically well resolved stratosphere and use the same KIE estimates for the oxidation of methane by OH, Cl and $O(^1D)$ as used in this study. The results from both models show a significant reduction in the methane mixing ratio and a concomitant increase in the $\delta^{13}C$ above the tropopause. The vertical structure of the methane fields in both model studies are consistent with our results when the eNIRVANA advection scheme is employed. The average mass weighted difference between the stratospheric and tropospheric $\delta^{13}C$ in the eNIRVANA configuration of our model is 1.9‰ which is qualitatively consistent with Bergamaschi et al. (1996) and McCarthy et al. (2003). This is not true of the model using the TVD advection scheme which shows a mass weighted average difference in $\delta^{13}C$ of less than 0.35‰.

Finally Brenninkmeijer et al. (1995) derive an overall KIE in the lower stratosphere of 12‰ based on measurements from air samples made in the lower stratosphere which again is consistent with our model results when the eNIRVANA advection scheme is used. The eNIRVANA model produces a KIE ranging between 9 and 16‰ within the same latitude range.

The stratospheric measurement and model comparisons discussed above strongly suggest that the model using the eNIRVANA advection scheme produces more realistic results than the model using the TVD scheme. This conclusion should be treated with some caution because the model configuration used here has few (∼6) levels in the stratosphere and therefore is not expected to model the stratospheric circulation particularly well and thus the improvements seen in changing from the TVD to the eNIRVANA schemes may be masking deficiencies in the dynamical model of stratosphere. Gregory and West (2002) and Eyring et al. (2006) show results from the stratospheric configuration of the UM and demonstrate that the stratospheric tape recorder and the mean age of air, respectively, are reasonably well modelled using the UM with the eNIRVANA advection scheme.

5. Conclusions

Two advection schemes have been tested within the UM general circulation model. The results suggest that the differences in the large-scale tracer distributions seen in the model results are strongly related to the different vertical transport speeds of the two schemes. Previous work (Gregory and West, 2002) showed that the TVD scheme is more diffusive than eNIRVANA, resulting in faster vertical transport of H_2O in the stratosphere. For long-lived tracers with a surface source such as the SF_6 experiment carried out here, this results in the TVD scheme producing lower mixing ratios in the lower and mid troposphere and higher mixing ratios in the stratosphere relative to the eNIRVANA scheme. Comparison with measurements and other model results suggest the model using the eNIRVANA scheme is producing more realistic results.

For chemically active species, the differences in the atmospheric distributions due to different advection schemes can be reduced by the atmospheric chemistry which can wield some control on the mixing ratios. In the CH_4 experiment, the effect of the OH chemistry almost completely removed any differences in mixing ratio in the middle and lower troposphere caused by changing from the TVD to the eNIRVANA advection scheme. In the stratosphere, where the advection dominates transport and the CH_4 loss rates themselves were parametrized, the equilibrium CH_4 mixing ratios were significantly different for the two advection schemes.

The equilibrium $\delta^{13}C$ values for the two advection schemes are different at all pressure levels considered here. The fact that the $\delta^{13}C$ values are different between the two advection schemes but the CH_4 mixing ratios themselves are not, reflects the fact that the $\delta^{13}C$ is a ratio metric of two chemically active species that are both influenced similarly (though not identically) by the OH chemistry in the model. The $\delta^{13}C$ is sensitive to the mean age of the CH_4, which in turn is influenced by the particular choice of the advection scheme.

The comparisons between the TVD and eNIRVANA results discussed here and the conclusions drawn apply to large spatial scales and temporal averages of the order of years and therefore apply to the large-scale structure of the tracer distributions. The results suggest that the differences in modelled surface mixing ratios and $\delta^{13}C$ for methane associated with the change in advection scheme at the Earth's surface are relatively small compared with differences introduced through uncertainties in the prescribed emissions.

A stringent test of a model's tracer advection scheme is comparison with measurements in the upper troposphere and stratosphere because in this region advection dominates the transport of long-lived species. The comparison of the modelled CH_4 mixing ratio and $\delta^{13}C$ profiles with the measurements of Sugawara et al. (1997) clearly demonstrates that the model using the eNIRVANA scheme produces more realistic CH_4 profiles than the same model using the TVD advection scheme. As discussed in Gregory and West (2002), this can be explained by the excessive numerical diffusion inherent in the TVD scheme. In this study, conclusions based on model results from the stratosphere must be treated with some caution because of the limited number of model levels in the stratosphere.

Smaller spatial scales and short time-scale variability have not been considered here but it is anticipated that conclusions about the differences between the two advection schemes would change when considering these smaller spatio-temporal scales. Previous comparisons of southern hemisphere MBL measurements with the model results (both the TVD and eNIRVANA) (Lowe et al., 2004; Allan et al., 2007) show that the seasonal cycles are well reproduced by both schemes. No detailed

measurement/model comparison of the daily variability at these sites has yet been carried out.

6. Acknowledgments

We thank Hilary Spencer (University of Reading) for providing the composite El Niño and La Niña SST data. We thank Sander Houweling (National Institute for Space Research, The Netherlands) for providing the GAMeS scenario fields. This work was supported by the New Zealand Foundation for Research, Science and Technology under contract C01X0204.

References

Allan, W., Lowe, D. C., Gomez, A. J., Struthers, H. and Brailsford, G. W. 2005. Interannual variation of ^{13}C in tropospheric methane: Implications for a possible atomic chlorine sink in the marine boundary layer. *J. Geophys. Res.* **110**(D11306), doi:10.1029/2004JD005650.

Allan, W., Struthers, H. and Lowe, D. C. 2007. Methane carbon isotope effects caused by atomic chlorine in the marine boundary layer: global model results compared with southern hemisphere measurements. *J. Geophys. Res.* **112**(D04306), doi:10.1029/2006JD007369.

Bergamaschi, P., Brühl, C., Brenninkmeijer, C. A. M., Saueressig, G., Crowlet, J. N., and co-authors. 1996. Implications of the large carbon kinetic isotope effect in the reaction $CH_4 + Cl$ for the $^{13}C/^{12}C$ ratio of stratospheric CH_4. *Geophys. Res. Lett.* **6**(14), 2227–2230.

Blackader, A. K. 1962. The vertical distribution of wind and turbulent exchange in a neutral atmosphere. *J. Geophys. Res.* **67**, 3095–3102.

Brasseur, G. P. and Solomon, S. 2005. *Aeronomy of the Middle Atmosphere*, (edsL. A. Mysak and K. Hamilton). Springer, Dordrecht, The Netherlands, 88–90.

Brenninkmeijer, C. A. M., Lowe, D. C., Manning, M. R., Sparks, R. J. and van Valthoven, P. F. J. 1995. ^{13}C, ^{14}C, and ^{18}O isotopic composition of CO, CH_4, and CO_2 in the higher southern-latitudes lower stratosphere. *J. Geophys. Res.* **100**, 26163–26172.

Craig, H. 1957. Isotopic standards for carbon and oxygen and correction factors for mass spectrometric analysis of carbon dioxide. *Geochim. Cosmochim. Acta* **12**, 133–149.

Cullen, M. J. P. 1993. The unified forecast/climate model. *Met. Mag.* **122**, 81–94.

Cullen, M. J. P. and Davis, T. 1991. A conservative split-explicit integration scheme with fourth-order horizontal advection. *Q. J. R. Meteorol. Soc.* **117**, 993–1002.

Cullen, M. J. P. and Barnes, R. T. H. 1997. Positive definite advection scheme. *Unifed Model Documentation Paper number 11*, 1–8.

Denning, A. S., Holzer, M., Gurney, K. R., Heimann, M., Law, R. M. and co-authors. 1999. Three-dimensional transport and concentration of SF_6: a model intercomparison study (TransCom2). *Tellus* **51B**, 266–297.

Eyring, V., Butchart, N., Waugh, D., Akiyoshi, H., Austin, J. and co-authors. 2006. Assessment of temperature, trace species, and ozone in chemistry-climate model simulations of the recent past. *J. Geophys. Res.* **111**(D22308), doi:10.1029/2006JD007327.

Finlayson-Pitts, B. J. and Pitts, J. N. 2000. *Chemistry of the Upper and Lower Atmosphere*, Academic Press, San Diego, California 92101-4495, USA, 658–659.

Fritsch, J. M. and Chappell, C. F. 1980. Numerical prediction of convectively driven mesoscale pressure systems. Part I : convective parameterization. *J. Atmos. Sci.* **37**, 1722–1733.

Godunov, S. K. 1959. A difference scheme for numerical computation of discontinuous solutions of equations in fluid dynamics. *Mat. Sb.* **4**, 271.

Gregory, A. R. and West, V. 2002. The sensitivity of a model's tape recorder to the choice of advection scheme. *Q. J. R. Meteorol. Soc.* **128**, 1827–1846.

Intergovernmental Panel on Climate Change 2001. In: *Climate Change 2001: the Scientific Basis*, (eds. J. T. Houghton *et al.*), Cambridge Univ. Press, New York.

Law, R. M., Rayner, P. J., Denning, A. S., Erickson, D., Heimann, M. and co-authors. 1996. Variations in modelled atmospheric transport of carbon dioxide and the consequences for CO_2 inversions. *Global Biogeochem. Cycles* **10**, 783–796.

Leonard, B. P. 1991. The ULTIMATE conservative difference scheme applied to unsteady one-dimensional advection. *Comput. Method Appl. Mech. Eng.* **88**, 17–74.

Leonard, B. P., Lock, A. P. and MacVean, M. K. 1995. The NIRVANA scheme applied to one-dimensional advection. *Methods Heat Fluid Flow* **5**, 341–377.

Levin, I. and Hesshaimer, V. 1996. Refining of atmospheric transport model entries by the globally observed passive tracer distributions of ^{85}Kr and sulphur hexafluoride (SF_6). *J. Geophys. Res.* **101**, 16745–16755.

Lowe, D. C., Koshy, K., Bromley, T., Allan, W., Struthers, H. and Maata, M. 2004. Seasonal cycles of mixing ratio and ^{13}C in atmospheric methane at Suva, Fiji. *J. Geophys. Res.* **109**(D23308), doi:10.1029/2004JD005166.

McCarthy, M. C., Boering, K. A., Rice, A. L., Tyler, S. C., Connell, P. and Atlas, E. 2003. Carbon and hydrogen isotopic compositions of stratospheric methane: 2. Two-dimensional model results and implications for kinetic isotope effects. *J. Geophys. Res.* **108**(D15), 4461, doi:10.1029/2002JD003183.

Mikaloff Fletcher, S. E., Tans, P. P., Bruhwiler, M., Miller, J. B. and Heimann, M. 2004. CH_4 sources estimated from atmospheric observations of CH_4 and its $^{13}C/^{12}C$ isotopic ratios: 1. Inverse modeling of source processes. *Global Biogeochem. Cycles* **18**, GB4004, doi:10.1029/2004GB002223.

National Oceanic and Atmospheric Administration 2001. GLOBALVIEW-CH_4: Cooperative Atmospheric Data Integration Project - Methane, report, Clim. Monit. and Diag. Lab., Boulder, Colo. (Also available at ftp.cmdl.noaa.gov, Path: ccg/ch4/GLOBALVIEW).

Pole, V. D., Gallani, M. L., Rowntree, P. R. and Stratton, R. A. 2000. The impact of new physical parameterizations in the Hadley Centre climate model: HadAM3. *Climate Dynamics* **16**, 123–146.

Prather, M., Ehhalt, D., Dentener, F., Derwent, R., Dlugokencky, E. and co-authors. 2001. Atmospheric chemistry and greenhouse gases. In: *Climate Change 2001: The Scientific Basis-Contribution of Working Group I to the Third Assessment Report of the Intergovernmental Panel on Climate Change* (eds J. Y. Houghton, *et al.*). Cambridge University Press, New York, 241–287.

Rasch, P. J., Mahowald, N. M. and Eaton, B. E. 1997. Representations of transport, convection and the hydrologic cycle in chemical transport models: Implications for the modeling of

short lived and soluble species. *J. Geophys. Res.* **102**, 28127–28138.

Rayner, P. J. and Law, R. M. 1995. A comparison of modelled responses to prescribed CO_2 sources. CSIRO Division of Atmospheric Research Technical Paper No. 36., 84pp.

Roe, P. L. 1985. Large scale computations in fluid mechanics. *Lectures in Applied Maths* **22**, 162pp.

Sander, S. P., Friedl, R. R., Golden, D. M., Kurylo, M. J., Huie, R. E. and co-authors. 2003. Chemical kinetics and photochemical data for use in atmospheric studies. Tech. Rep. Evaluation 14, Jet Propulsion Laboratory, Pasadena, CA.

Saueressig, G., Crowley, J. N., Bergamaschi, P., Brühl, C., Brenninkmeijer, C. A. M. and co-authors. 2001. Carbon 13 and D kinetic isotope effects in the reactions of CH_4 with $O(^1D)$ and OH: New laboratory measurements and their implications for the isotopic composition of stratospheric methane. *J. Geophys. Res.* **106**, 23127–23138.

Smith, R. N. B. 1993. Subsurface, surface and boundary layer processes. *Unifed Model Documentation Paper number 24* 1.33–1.37.

Spencer, H., Slingo, J. M. and Davey, M. K. 2004. Seasonal predictability of ENSO teleconnections: The role of the remote ocean response. *Climate Dynamics* **22**, 511–526, doi:10.1007/s00382-004-0393-1.

Sugawara, S., Nakazawa, T., Shirakawa, Y., Kawamura, K., Aoki, S., and co-authors. 1997. Vertical profile of the carbon isotopic ratio of stratospheric methane over Japan. *Geophys. Res. Lett.* **24**(23), 2989–2992.

van Leer, B. 1977. Towards the ultimate conservative difference scheme IV. A new approach to numerical advection. *J. Comp. Phys.* **23**, 276–299.